Journal of Guidance, Control, and Dynamics
Vol. 30, No. 6, November–December 2007

Analytical Charge Analysis for Two- and Three-Craft Coulomb Formations

John Berryman* and Hanspeter Schaub†
Virginia Polytechnic Institute and State University, Blacksburg, Virginia 24061-0203

DOI: 10.2514/1.23785

For close-proximity flying on the order of 10–100 m, Coulomb thrusting presents a promising alternative to other methods of propulsion. This clean and fuel-efficient propulsion method is being investigated for use in formation flying and virtual structures. In the latter application, the individual spacecraft assume fixed positions relative to one another through the use of Coulomb forces. This paper provides an analytical investigation of static Coulomb formations. The open-loop, constant charges necessary to support a Hill-frame stationary formation are analytically determined for two- and three-craft formations. These static formations are relative equilibriums of the charged relative orbits. Applying the necessary conditions regarding the formation center-of-mass and principal inertias, closed-form charge solutions are developed for linear two-craft formations, as well as linear and equilateral triangle three-craft geometries. The orientations for which the required spacecraft charges are real and constant are investigated. Finally, a general method is outlined to compute required products of spacecraft charges for a formation of *N* craft.

I. Introduction

CURRENTLY, the aerospace community is recognizing more and more applications for close-proximity formation flying with separation distances varying between 10–100 m. The ideas include plans for sparse aperture interferometry to provide remote surveillance of the Earth, and plans for spacecraft to circumnavigate and diagnose damaged spacecraft and repair them. However, there remain several technological and logistical obstacles before such missions can be realized. Coulomb control is steadily gaining attention as an approach for controlling close-proximity formations. The premise of Coulomb thrusting is to control the electrostatic charge of spacecraft. The resulting intervehicular forces are thereby used to control the shape and size of the spacecraft formation. Geosynchronous Earth orbit (GEO) spacecraft naturally acquire absolute charge levels on the order of kilovolts due to their interaction with the tenuous plasma environment. As a result, without charge control, these natural electrostatic forces can cause a close 20 m formation to experience hundreds of meters of separation over a GEO orbit. The concept of Coulomb thrusting controls the absolute spacecraft charge to create desired Coulomb forces. To control the spacecraft charge, an electric field is used to accelerate positive ions and negative electrons such that they escape from the spacecraft. Missions showing the feasibility of active charge control include SCATHA [1] and ATS [2] in which the craft were actively charged to nonzero potentials, as well as the more recent Equator-S [3], Geotail [4], and CLUSTER [5] missions which servo the spacecraft charge to zero. The required charge magnitudes for Coulomb thrusting depends on the formation size and geometry. For the concepts considered here, the charge levels range from 1–10 kV, which is similar to the naturally occurring electrostatic charge levels or the active charging demonstrated on the SCATHA and ATS missions. With specific impulses as high as 10^{13} s, Coulomb control is orders of magnitude more fuel efficient than other forms of propulsion currently being considered for close-proximity formation flying. The high fuel-efficiency and dependence upon renewable energy will allow Coulomb formations to have mission lives considerably longer than electric propulsion based formations.

Electric propulsion (EP) thrusters have been considered as a candidate technology for close-proximity flying on the order of 10–100 m, however, there are several problems associated with this method of propulsion that may ultimately prove insurmountable. The basic concept of the EP thruster is to rapidly accelerate and eject charged particles and, in doing so, propel the spacecraft forward. This method of propulsion has many beneficial qualities. For instance, the specific impulse I_{sp} provided by these systems takes values up to 6000 s. Additionally, the total mass of EP systems is often just a fraction of the mass of more traditional propulsion systems. Unfortunately, EP systems have one significant drawback for close-proximity missions: the charged particles that they emit are caustic and tend to damage any material they contact. In single-spacecraft missions, this effect is of no consequence because the propellant is discharged safely behind the spacecraft. However, when several spacecraft are in close proximity with one another, the propellant can damage the fragile components of nearby spacecraft. Also, because EP systems expel matter as a source of propulsion, the life of a mission will often be limited by the amount of propellant that can be carried aboard a spacecraft [6]. Unlike electric propulsion systems, the Coulomb propulsion concept is essentially propellant-less [6,7], and thus there is little danger of equipment damage due to plume impingement.

Applications of Coulomb formations vary widely. One important application is sparse radar or optical interferometry. King et al. [7] discuss a novel method of achieving wide field-of-view interferometry using Coulomb thrusting. Using a distributed set of sensors, discrete readings are combined to form a high-resolution image. Meter-level sensing accuracy with infinite dwell time could be achieved by having sensors flying tens of meters apart at geostationary altitudes to form a sparse interferometric dish. In contrast, building a single structure with a diameter ranging from tens to hundreds of meters would be a costly and challenging endeavor. Interferometry, especially optical interferometry, requires very precise alignment of the sensors. Adequately controlling the vibration and flexing modes of large monolithic structures would be a difficult task. Instead, distributing sensors discretely in a tight formation would provide an attractive alternative. Such formations

Received 28 November 2006; revision received 30 May 2007; accepted for publication 31 May 2007.

*Graduate Student, Aerospace and Ocean Engineering Department, Virginia Polytechnic Institute and State University, Blacksburg, VA 24061-0203.

†Assistant Professor, Virginia Polytechnic Institute and State University, Blacksburg, VA 24061-0203.

would be more robust to single sensor failures, because the formation could continue to function at a reduced capacity (whereas a large dish, for example, might afterward be inoperable). Another application of the Coulomb concept is discussed by Natarajan and Schaub in [8]. In this paper, the authors discuss the concept of a virtual Coulomb tether. Here a physical tether or boom between two spacecraft is replaced with an electrostatic force field. This basic concept could eventually be expanded so that entire virtual structures could be constructed using electrostatic forces rather than a physical truss system as internal support. Further applications include advanced docking mechanisms, autonomous inspection craft capable of circumnavigating a spacecraft via electrostatic forces, and sparse vehicles capable of carrying hazardous materials in tow without any physical contact through the use of intercraft Coulomb forces.

Even though Coulomb control enjoys obvious advantages, it also provides some challenges. Coulomb control is based upon the attraction and repulsion of charged bodies. For this reason, the charged plasma environment in space tends to diminish the electrostatic influence of one spacecraft upon another by masking their charges. This is typically quantified through the plasma Debye length [9]. Additionally, all forces are internal with Coulomb control, i.e., each satellite is either pushing or pulling against the others. Therefore, the inertial linear and angular momentum of a formation can not be directly altered by Coulomb forces [10,11]. Finally, the dynamics of a Coulomb spacecraft are highly coupled and nonlinear. For example, if the position or charge of one spacecraft is altered, the forces on all spacecraft are affected. Despite the difficulties inherent to Coulomb control, if the dynamics are better understood, then Coulomb control might one day provide a fuel-efficient, inexpensive, long-lasting, and dependable method for controlling close-proximity formations.

Although the concept of Coulomb formation control is relatively new, there have already been several papers published that attest to its feasibility in real-life application. The initial NASA Institute for Advanced Concepts (NIAC) report by King et al. [7], remains one of the most comprehensive investigations of Coulomb control for spacecraft formations. This report contains a wide range of information including methods for physically implementing Coulomb control, potential applications of Coulomb formations, analytical derivations for several static and dynamic formations, and comparison of Coulomb propulsion with existing technologies. In [12], Schaub et al. investigate examples of new analytical static Coulomb formations, discuss open-loop instability of such formations, and develop an orbit element difference-based feedback control law to stabilize relative motion between two craft. In [8], Natarajan and Schaub present a method of implementing and stabilizing a Coulomb tether. Here, a nadir-pointing, two-craft formation maintains a fixed separation distance while exploiting gravity gradient torque to stabilize the formation attitude. Necessary conditions are developed in [13] for static, constant-charge, Coulomb formations. Here, a Hamiltonian formulation is used to analyze the dynamics of a Coulomb formation in a manner analogous to the analysis of a rigid body. In [14,15], charge feedback control strategies are explored in which a sensor craft is positioned using multiple drone craft.

This paper discusses analytical charge solutions to create a static Coulomb formation. Here the spacecraft positions and charges are chosen such that the Coulomb forces cancel any differential gravitational forces. This results in the spacecraft cluster remaining static with respect to the rotating center-of-mass frame. These geometries are relative equilibriums of the charged relative motion. Of particular concern is that the required charge solutions must be both real and constant. A constant-charge solution (vs a solution which modulates between two different charge levels) requires much less electrical power to implement and is thus more feasible for small spacecraft applications. Determining the equilibrium charges necessary to implement a static Coulomb formation is very important because the charge solutions can then be used as open-loop, feed-forward charges in stabilizing feedback control laws. These open-loop, static Coulomb formation solutions are unstable without feedback. The main impetus of this paper is to determine all analytical charge solutions for two- and three-craft static formations, and investigate issues with scaling these solutions to formations with more craft. Previous work only provided analytical solutions for very particular symmetric formations [7], or used numerical methods to determine feasible charged static formations [16].

In the problem statement of this paper, the fundamental concepts that drive the analysis are introduced. This section includes conditions that must be satisfied to ensure that a Coulomb formation remains static, as well as the necessary conditions that must be imposed upon the formation center-of-mass and principal axes. The center-of-mass and principal axes conditions become important in finding analytical solutions to the static equations.

The analysis of static Coulomb formations begins with a tutorial case of a two-spacecraft formation. Here a notational system is introduced which simplifies the remaining analysis by allowing all possible orientations of a formation to be considered simultaneously. This section also introduces the concept of solving for the products of the interspacecraft charges (hereafter termed "charge products"), rather than directly solving for the charges themselves.

The analysis is then extended to the more complicated case of three-spacecraft formations. Initially, the three-craft formations considered are aligned with one of the Hill-frame axes. This analysis introduces necessary conditions which must be fulfilled by the charge products to ensure that the Coulomb formations can be implemented with static charges. The analysis continues with arbitrary triangular formations. After a brief overview of considerations for this more general case, the analysis turns to a specific example of a triangular formation: the equal-mass, equilateral formation.

The remaining analysis investigates extending these concepts to the general case of N-craft static Coulomb formations. The N-craft study does not yield complete charge solutions for static formations. Instead, this study investigates how the three-craft charge implementation issues scale to the N-craft cases.

II. Problem Statement

Let $\boldsymbol{r}_i$ represent the inertial position of the ith spacecraft within a formation. Also, let $\boldsymbol{r}_c$ represent the inertial position vector of the center of mass of a spacecraft formation. The position of the spacecraft relative to the formation center of mass is then $\boldsymbol{\rho}_i = \boldsymbol{r}_i - \boldsymbol{r}_c$ and the position of spacecraft i relative to spacecraft j is similarly defined as $\boldsymbol{\rho}_{ji} = \boldsymbol{\rho}_i - \boldsymbol{\rho}_j$. The Hill frame is defined as $\mathcal{H}$: $\{\mathcal{O}, \hat{\boldsymbol{o}}_r, \hat{\boldsymbol{o}}_\theta, \hat{\boldsymbol{o}}_h\}$, where $\hat{\boldsymbol{o}}_r$ points radially away from the center of Earth, $\hat{\boldsymbol{o}}_h$ points in the orbit-normal direction, and the final unit vector $\hat{\boldsymbol{o}}_\theta$ completes the triad such that $\hat{\boldsymbol{o}}_\theta = \hat{\boldsymbol{o}}_h \times \hat{\boldsymbol{o}}_r$. For circular restricted center-of-mass motion considered in this research, $\hat{\boldsymbol{o}}_\theta$ is always in the direction of the velocity of the formation center of mass. As illustrated in Fig. 1, the ith relative position vector is represented in the Hill-frame vector components as

$$\boldsymbol{\rho}_i = {}^{\mathcal{H}}\begin{bmatrix} x_i \\ y_i \\ z_i \end{bmatrix} \tag{1}$$

Under the assumption that the formation spacecraft are point charges, if each spacecraft has a charge q_i, then the Coulomb interaction between the ith and jth spacecraft is proportional to the product of their charges and inversely proportional to the square of their separation distance. If the charges are of like sign, then the

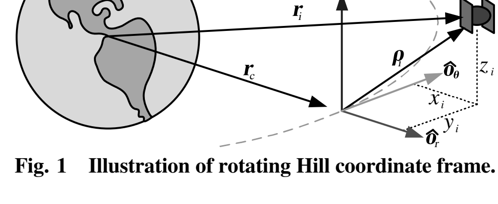

Fig. 1 Illustration of rotating Hill coordinate frame.

interaction is repulsive; otherwise it is attractive. The equations of motion for a Coulomb spacecraft formation can be found by including the Coulomb acceleration term on the right side of the Hill's equations [17–19].

$$\ddot{x}_i - 2n\dot{y}_i - 3n^2 x_i = \frac{k_c}{m_i}\sum_{j=1}^{N}\frac{x_i - x_j}{\rho_{ji}^3} q_i q_j e^{-\frac{\rho_{ij}}{\lambda_d}} \tag{2a}$$

$$\ddot{y}_i + 2n\dot{x}_i = \frac{k_c}{m_i}\sum_{j=1}^{N}\frac{y_i - y_j}{\rho_{ji}^3} q_i q_j e^{-\frac{\rho_{ij}}{\lambda_d}} \tag{2b}$$

$$\ddot{z}_i + n^2 z_i = \frac{k_c}{m_i}\sum_{j=1}^{N}\frac{z_i - z_j}{\rho_{ji}^3} q_i q_j e^{-\frac{\rho_{ij}}{\lambda_d}} \tag{2c}$$

Here n refers to the mean orbit rate for motion of the center of mass, and k_c refers to Coulomb's constant, $8.99 \times 10^9\ \mathrm{Nm^2/C^2}$. Note that the orbital motion has been linearized, whereas the Coulomb force is left in its full nonlinear form. The exponential term on the right-hand side of Eqs. (2) dictates the rate at which the Coulomb influence decays with increasing distance in a plasma environment. This decay is a function of the Debye length λ_d and is due to the shielding effect that is created around a charged body when submersed in a plasma environment [9]. In low Earth orbit (LEO), the Debye length can be on the order of centimeters, rendering this method of control ineffective except at extremely close ranges, for example, small corrections during the final phase of docking. On the other hand, at geosynchronous Earth orbit (GEO) altitudes, the Debye length ranges from 140–1400 m [6,7]. Therefore, the initial portion of the analysis presented here considers GEO altitude formations with spacecraft separations on the order of 10 m. With such formations, the exponential term can be disregarded, so that the analysis parallels earlier methods used by King et al. to find analytical charge solutions [7].

For the spacecraft to remain fixed relative to the Hill frame, all derivatives in Eqs. (2) must remain zero for all time. This relative equilibrium configuration is achieved by carefully placing and charging the craft such that the Hill-frame accelerations are canceled by the accelerations due to Coulomb forces. These equilibriums are unstable without feedback. An example of a feedback stabilized, two-craft static Coulomb formation is the Coulomb tether concept in [20]. Determining relative equilibria solutions of Eqs. (2) with constant-charge solutions is nontrival. A static Coulomb formation of N craft must satisfy $3N$ relative equilibrium conditions in Eqs. (2). Each spacecraft can select three position degrees of freedom (x_i, y_i, z_i) and the spacecraft charge q_i to cancel the Hill-frame accelerations.

To make the analysis less complicated, the equations of motion are scaled with respect to the orbital rate n and Coulomb's constant k_c. This scaling is accomplished by introducing a scaled charge $\tilde{q} \equiv q\sqrt{k_c}/n$. By substituting in this new variable, disregarding the exponential term and setting all derivatives to zero, the static equations for a Coulomb formation can be written as

$$m_i\frac{\ddot{x}_i}{n^2} = 0 = 3x_i m_i + \sum_{j=1}^{N}\frac{x_i - x_j}{\rho_{ji}^3}\tilde{q}_i\tilde{q}_j \tag{3a}$$

$$m_i\frac{\ddot{y}_i}{n^2} = 0 = \sum_{j=1}^{N}\frac{y_i - y_j}{\rho_{ji}^3}\tilde{q}_i\tilde{q}_j \tag{3b}$$

$$m_i\frac{\ddot{z}_i}{n^2} = 0 = -z_i m_i + \sum_{j=1}^{N}\frac{z_i - z_j}{\rho_{ji}^3}\tilde{q}_i\tilde{q}_j \tag{3c}$$

If these equations are satisfied for a Coulomb formation, then the Hill-frame accelerations are exactly matched by the Coulomb accelerations and the spacecraft remain fixed in place with respect to the Hill frame. Notice in Eqs. (3) that the equations are linear in the charge products $\tilde{q}_i\tilde{q}_j$. This fact is central to the analytical treatment, and for this reason we represent the charge products as Q_{ij} as follows:

$$Q_{ij} \equiv \tilde{q}_i\tilde{q}_j \tag{4}$$

A Hill-frame static formation must satisfy two necessary conditions [13]. The first condition is that the formation center of mass must be located at the origin of the Hill frame and the second is that the principal axes of the formation must be aligned with the axes of the Hill frame.

First, the center-of-mass condition is considered. If the formation remains rigid, then the center of mass of the formation moves according to Hill's equations as presented in Eqs. (2), except that there is no forcing function and the right-hand side of the equation is therefore zero. Solving for the center-of-mass accelerations and prescribing the velocities to be zero yields

$$\ddot{x}_{\mathrm{cm}} = 3n^2 x_{\mathrm{cm}} \tag{5a}$$

$$\ddot{y}_{\mathrm{cm}} = 0 \tag{5b}$$

$$\ddot{z}_{\mathrm{cm}} = -n^2 z_{\mathrm{cm}} \tag{5c}$$

From Eqs. (5), it is apparent that if the center of mass is placed with nonzero x_{cm} and z_{cm} then there is an associated acceleration and the center of mass does not remain stationary. On the other hand, from Eq. (5b), if the center of mass only has an along-track displacement y_{cm}, then there is no associated acceleration and the center of mass remains stationary. This is the traditional leader–follower scenario of formation flying. This simple, chargeless formation is not unique. To avoid repeated solutions which only differ through a shift in the along-track direction $\hat{\boldsymbol{o}}_\theta$, the center of mass may not be offset in the $\hat{\boldsymbol{o}}_\theta$ direction. The center-of-mass condition is expressed mathematically as

$$M\boldsymbol{\rho}_{\mathrm{cm}} = \sum_{i=1}^{N} m_i\boldsymbol{\rho}_i = \sum_{i=1}^{N} m_i\begin{bmatrix} x_i \\ y_i \\ z_i \end{bmatrix} = \mathbf{0} \tag{6}$$

where M is the total mass of the formation, $\boldsymbol{\rho}_{\mathrm{cm}}$ is the position vector from the spacecraft to the center of mass, and all vector components are expressed with respect to the Hill frame.

The principal axes condition is now considered. A detailed study is found in [13]. For a formation whose center-of-mass motion is circularly restricted, a necessary relative equilibria condition is for the formation principal inertia axes to line up with the Hill-frame axes. This is the equivalent result typically used in determining rigid body satellite equilibrium conditions with the gravity gradient torque [19]. If this condition is not satisfied, then the resulting gravity gradient torque acting on this static formation will cause it to rotate and violate the static Hill-frame requirement. Because the desired static formations do not move with respect to the Hill frame, the Hill-frame representation of the formation inertia matrix is constant and can be defined as

$$[I] \equiv {}^{\mathcal{H}}\begin{bmatrix} I_{xx} & I_{xy} & I_{xz} \\ I_{xy} & I_{yy} & I_{yz} \\ I_{xz} & I_{yz} & I_{zz} \end{bmatrix} = \sum_{i=1}^{N} m_i\, {}^{\mathcal{H}}\begin{bmatrix} y_i^2 + z_i^2 & -x_i y_i & -x_i z_i \\ -x_i y_i & x_i^2 + z_i^2 & -y_i z_i \\ -x_i z_i & -y_i z_i & x_i^2 + y_i^2 \end{bmatrix} \tag{7}$$

Because the formation principal axes must be aligned with the Hill-frame axes, the formation inertia matrix must be a diagonal. The principal axes condition for a static charged formation then requires that the formation craft are placed such that the resulting formation inertia matrix off-diagonal terms are zero:

$$I_{xy} = -\sum_{i=1}^{N} m_i x_i y_i = 0 \tag{8a}$$

$$I_{yz} = -\sum_{i=1}^{N} m_i y_i z_i = 0 \tag{8b}$$

$$I_{zx} = -\sum_{i=1}^{N} m_i z_i x_i = 0 \tag{8c}$$

In summary, to maintain a unique, static formation in the Hill frame, it has been shown that the formation center of mass must be located at the origin of the Hill frame and the formation principal axes must be aligned with the Hill-frame axes. However, these are simply necessary and not sufficient conditions for a constant-charge static Coulomb formation. As is discussed in the following section, it is possible to place the craft such that the formation center-of-mass and principal inertia conditions are satisfied, only to find that the required spacecraft charges must be imaginary.

III. Analysis of a Two-Spacecraft Formation

This section provides an analysis of a static formation with two spacecraft. The section also serves as a tutorial for a new notational convention used through the remainder of this paper which decreases work necessary for the analysis by allowing several cases to be considered simultaneously.

A. Two-Spacecraft Formation Aligned with $\hat{\boldsymbol{o}}_r$ Axis

Figure 2 shows two spacecraft aligned with the orbit radial axis $\hat{\boldsymbol{o}}_r$. Note that this simple formation inherently satisfies the principal axis condition. They are separated by a distance L and in accordance with the center-of-mass condition, the formation center of mass is located at the Hill-frame origin. Using the center-of-mass condition, the position of the second mass is expressed in terms of the first mass's position through

$$x_2 = -\frac{m_1}{m_2} x_1 \tag{9}$$

The separation distance is then expressed in terms of the first position as

$$L = x_2 - x_1 = -x_1\left(1 + \frac{m_1}{m_2}\right) \tag{10}$$

To cancel the Hill-frame accelerations in Eq. (3a), there are two equations that must be satisfied for each spacecraft to be stationary:

$$-3x_1 = \frac{1}{m_1}\frac{x_1 - x_2}{L^3}\tilde{q}_1\tilde{q}_2 = -\frac{Q_{12}}{m_1 L^2} \tag{11a}$$

$$-3x_2 = \frac{1}{m_2}\frac{x_2 - x_1}{L^3}\tilde{q}_1\tilde{q}_2 = \frac{Q_{12}}{m_2 L^2} \tag{11b}$$

where $Q_{ij} \equiv \tilde{q}_i\tilde{q}_j$. By substituting the center-of-mass condition of Eq. (9) into Eq. (11b), it is trivial to show that Eq. (11b) is redundant, and Eq. (11a) is then the only necessary condition. Solving this equation for the charge product Q_{12} yields

$$Q_{12} = 3m_1 x_1 L^2 = -3L^3 \frac{m_1 m_2}{m_1 + m_2} \tag{12}$$

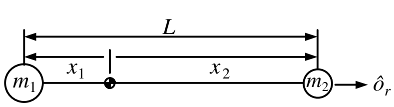

Fig. 2 Two-spacecraft formation aligned with the $\hat{\boldsymbol{o}}_r$ axis.

If the spacecraft charges satisfy Eq. (12), then the formation remains stationary in the Hill frame.

B. Introduction of New Notation

It may seem that similar solutions to the two-craft nadir-aligned case can be found for arbitrary placement of two spacecraft as long as the center-of-mass condition is satisfied. However, to maintain a static Coulomb formation, the formation principal axes must be aligned with the axes of the Hill frame. Rather than replicating the previous analysis for all possible two-spacecraft alignments, a notational system is introduced that allows the simultaneous development of all solutions.

Instead of examining positions x_i along the $\hat{\boldsymbol{o}}_r$ axis, the premise of the following notational system is to examine positions d_i along an unspecified axis $\hat{\boldsymbol{o}}_1$ that can be chosen from $\hat{\boldsymbol{o}}_r$, $\hat{\boldsymbol{o}}_\theta$, or $\hat{\boldsymbol{o}}_h$. Using this notation, Eqs. (3) can be rewritten as

$$a_d d_i = \frac{1}{m_i}\sum_{j=1}^{N}\frac{d_i - d_j}{\rho_{ji}^3}\tilde{q}_i\tilde{q}_j \tag{13}$$

where a_d is a constant that depends upon the choice of d. If $d = x$, then $a_d = a_x = -3$; if $d = y$, then $a_d = a_y = 0$; finally, if $d = z$, then $a_d = a_z = 1$. This equation is equivalent to Eqs. (3) yet it allows the direction in which distances are measured to remain arbitrary. Using this notation, Eq. (13) can be solved for the charge products Q_{ij}. By then supplying the appropriate value for the constant a_d, the results can then be specified for a two-craft formation aligned with any Hill-frame axis.

C. Two-Spacecraft Formation Aligned with Any Hill-Frame Axis

Making use of the notation just presented, the necessary condition represented in Eq. (11a) can be generalized to

$$a_d d_1 = \frac{1}{m_1}\frac{d_1 - d_2}{L^3}\tilde{q}_1\tilde{q}_2 = -\frac{Q_{12}}{m_1 L^2} \tag{14}$$

Solving for the required charge product for a static two-craft solution yields

$$Q_{12} = -a_d m_1 d_1 L^2 = a_d L^3 \frac{m_1 m_2}{m_1 + m_2} \tag{15}$$

Several conclusions can be drawn from this general equation by substituting in values for the constant a_d. If the formation is aligned with the $\hat{\boldsymbol{o}}_r$ axis, then $a_d = a_x = -3$. Because the separation distance L and the masses are always positive, Q_{12} is negative and both spacecraft must be charged with opposite polarity. For the $\hat{\boldsymbol{o}}_\theta$ aligned case, $a_d = a_y = 0$; therefore, at least one craft must have zero charge so that there is no interaction between the two spacecraft. This formation corresponds to a leader–follower spacecraft formation, and any interspacecraft forces would clearly disrupt such a formation. Finally, if the spacecraft are aligned with $\hat{\boldsymbol{o}}_h$, then $a_d = a_z = 1$. In this case, the necessary charge product Q_{12} is a third of the charge product required for the $\hat{\boldsymbol{o}}_r$ aligned case; additionally, the spacecraft must be charged to the same polarity to support a stationary formation. The rationale behind this charging scheme can be understood by imagining the motion of two bodies whose orbits differ only in inclination. With no charge, the spacecraft would collide when they reached the equatorial plane; however, when charged to the same polarity, they push one another apart and do not collide.

Coulomb formations of two spacecraft are the simplest possible formations. Such formations will find utility as virtual tethers between two spacecraft [8] and for applications such as rendezvous and docking.

IV. Analysis of Linear Three-Spacecraft Formation

The same methodology is now applied to the analysis of a formation composed of three collinear spacecraft as illustrated in Fig. 3. Because of the principal axis constraint [13], linear formations

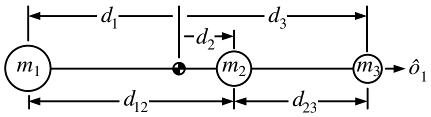

Fig. 3 Three-spacecraft formation aligned with an arbitrary axis.

must always be aligned with one of the three Hill-frame axes. In Fig. 3, the spacecraft are positioned along an arbitrary axis $\hat{\boldsymbol{o}}_1$ at locations d_1, d_2, and d_3, with separations of d_{12} and d_{23}.

For this formation, Eq. (13) is rewritten as three necessary conditions for a stationary formation:

$$a_d d_1 m_1 = \frac{d_1 - d_2}{d_{12}^3} Q_{12} + \frac{d_1 - d_3}{d_{13}^3} Q_{13} = -\frac{Q_{12}}{d_{12}^2} - \frac{Q_{13}}{d_{13}^2} \tag{16a}$$

$$a_d d_2 m_2 = \frac{d_2 - d_1}{d_{12}^3} Q_{12} + \frac{d_2 - d_3}{d_{23}^3} Q_{23} = \frac{Q_{12}}{d_{12}^2} - \frac{Q_{23}}{d_{23}^2} \tag{16b}$$

$$a_d d_3 m_3 = \frac{d_3 - d_2}{d_{23}^3} Q_{23} + \frac{d_3 - d_1}{d_{13}^3} Q_{13} = \frac{Q_{23}}{d_{23}^2} + \frac{Q_{13}}{d_{13}^2} \tag{16c}$$

Notice that Eqs. (16) are linear in the charge products Q_{ij}. Adding Eqs. (16a) and (16c) and substituting in the center-of-mass definition produces an equation identical to Eq. (16a). In effect, there are three variables available for control and only two independent necessary conditions. Therefore, one of the charge products, Q_{13} for example, may be chosen arbitrarily whereas the other charge products can be solved for from Eqs. (16a) and (16c):

$$Q_{12} = \left[-a_d d_1 m_1 - \frac{Q_{13}}{d_{13}^2}\right] d_{12}^2 \tag{17a}$$

$$Q_{23} = \left[a_d d_3 m_3 - \frac{Q_{13}}{d_{13}^2}\right] d_{23}^2 \tag{17b}$$

By considering the center-of-mass constraint, these equations are conveniently rewritten in terms of separation distances

$$Q_{12} = \left[\frac{a_d m_1}{M}[d_{12}(m_2 + m_3) + d_{23}(m_3)] - \frac{Q_{13}}{d_{13}}\right] d_{12}^2 \tag{18a}$$

$$Q_{23} = \left[\frac{a_d m_3}{M}[d_{12}(m_1) + d_{23}(m_1 + m_2)] - \frac{Q_{13}}{d_{13}}\right] d_{23}^2 \tag{18b}$$

where M is the total formation mass. With these equations, it is possible to determine the charge products necessary for a stationary, linear three-craft formation. However, it must be noted that although it is always be possible to determine the charge products Q_{ij}, it is not always possible to determine suitable individual spacecraft charges $\tilde{q}_i$. Using the definition of the charge product, $Q_{ij} = \tilde{q}_i \tilde{q}_j$, the individual charges are determined by solving for q_i as follows

$$\tilde{q}_i = \sqrt{\left(\frac{Q_{ij} Q_{ik}}{Q_{jk}}\right)} \tag{19}$$

Equation (19) implies two important qualities that must be exhibited by the charge products:

1) For the charges to be real quantities, the term under the radical must not be negative. However, rather than ensuring that $Q_{12}Q_{13}/Q_{23}$, $Q_{12}Q_{23}/Q_{13}$, and $Q_{13}Q_{23}/Q_{12}$ are not negative, it is equivalent to ensure that the triple product $Q_{12}Q_{23}Q_{13}$ is nonnegative.

2) For charge magnitudes to be finite, the value of $Q_{ij}Q_{jk}/Q_{ik}$ must be finite. Therefore, it is not possible to have a static formation when a single charge product Q_{ij} is zero because the denominator would be zero and the value for one of the charges $\tilde{q}_i$ would be infinite. However, because there are two charge products in the numerator, a static formation is still possible when either two or three charge products have zero value.

It should be possible to implement any linear three-spacecraft formation. However, the charge product Q_{13} must be carefully chosen such that these conditions are fulfilled. Just as in the case of two-spacecraft Coulomb formations, three-spacecraft formations may be used as virtual tethers, however, there currently exists no extensive stability or control analysis as in the case of nadir-pointing two-spacecraft formations.

V. Analysis of Triangular Three-Spacecraft Formations

A. Arbitrary Triangle Formation

An arbitrary, triangular, three-spacecraft formation must satisfy the conditions of Eqs. (3) which state that each craft must remain motionless in the $\hat{\boldsymbol{o}}_r$, $\hat{\boldsymbol{o}}_\theta$, and $\hat{\boldsymbol{o}}_h$ directions. These equations can be immediately reduced to six equations by recognizing that a three-craft formation is inherently planar and that one principal axis of any planar formation is perpendicular to the plane of the formation. Therefore, to satisfy the principal axes condition, the three spacecraft must lie in one of the three planes that are perpendicular to the Hill-frame axes. Because the formation spacecraft are constrained to lie in a plane spanned by two of the Hill-frame axes, it is unnecessary to include equations concerning motion perpendicular to this plane. The position of each spacecraft is then specified by two values: a distance d_i in the $\hat{\boldsymbol{o}}_1$ direction, and a distance e_i in the $\hat{\boldsymbol{o}}_2$ direction, where $\hat{\boldsymbol{o}}_1$ and $\hat{\boldsymbol{o}}_2$ can be defined as any combination of the directions $\hat{\boldsymbol{o}}_r$, $\hat{\boldsymbol{o}}_\theta$, and $\hat{\boldsymbol{o}}_h$. The remaining acceleration equations that must be satisfied for static formations are

$$m_i \frac{\ddot{d}_1}{n^2} = 0 = a_d m_1 d_1 + \frac{d_1 - d_2}{\rho_{12}^3} Q_{12} + \frac{d_1 - d_3}{\rho_{13}^3} Q_{13} \tag{20a}$$

$$m_i \frac{\ddot{d}_2}{n^2} = 0 = a_d m_2 d_2 + \frac{d_2 - d_1}{\rho_{12}^3} Q_{12} + \frac{d_2 - d_3}{\rho_{23}^3} Q_{23} \tag{20b}$$

$$m_i \frac{\ddot{d}_3}{n^2} = 0 = a_d m_3 d_3 + \frac{d_3 - d_1}{\rho_{13}^3} Q_{13} + \frac{d_3 - d_2}{\rho_{23}^3} Q_{23} \tag{20c}$$

$$m_i \frac{\ddot{e}_1}{n^2} = 0 = a_e m_1 e_1 + \frac{e_1 - e_2}{\rho_{12}^3} Q_{12} + \frac{e_1 - e_3}{\rho_{13}^3} Q_{13} \tag{20d}$$

$$m_i \frac{\ddot{e}_2}{n^2} = 0 = a_e m_2 e_2 + \frac{e_2 - e_1}{\rho_{12}^3} Q_{12} + \frac{e_2 - e_3}{\rho_{23}^3} Q_{23} \tag{20e}$$

$$m_i \frac{\ddot{e}_3}{n^2} = 0 = a_e m_3 e_3 + \frac{e_3 - e_1}{\rho_{13}^3} Q_{13} + \frac{e_3 - e_2}{\rho_{23}^3} Q_{23} \tag{20f}$$

The first derivatives are not included in these equations because they can be prescribed and will always be prescribed to zero for a static formation. The constants a_d and a_e are used to maintain generality and can be replaced by either -3, 0, or 1 depending upon the axial alignment of the formation. For instance, if the formation lies in the plane spanned by the vectors $\hat{\boldsymbol{o}}_r$ and $\hat{\boldsymbol{o}}_h$, then $a_d = a_x = -3$ and $a_e = a_z = 1$.

For an arbitrary three-craft formation, the center-of-mass condition applies two constraints that ensure the formation center of mass coincides with the origin of the Hill frame.

$$m_1 d_1 + m_2 d_2 + m_3 d_3 = 0 \tag{21a}$$

$$m_1 e_1 + m_2 e_2 + m_3 e_3 = 0 \tag{21b}$$

Similarly, the principal axes condition applies one more constraint to ensure that the product of inertia I_{de} is zero. If all products of inertia are zero, then all of the formation principal axes will be aligned with the Hill-frame axes. The principal axes constraint is

$$m_1 d_1 e_1 + m_2 d_2 e_2 + m_3 d_3 e_3 = 0 \tag{22}$$

The three constraints reduce the number of independent equations in Eqs. (20) from six to three. The center-of-mass condition in Eqs. (21) is used to eliminate the $\ddot{d}_3$ and $\ddot{e}_3$ conditions in Eqs. (20c) and (20f). The principal axis condition is used to eliminate the $\ddot{e}_2$ condition in Eq. (20e). The remaining three linearly independent equations in Eqs. (20) are used to determine the required charge products.

B. Equilateral Triangle Formation

The analysis just presented for arbitrary triangular formations is applicable for the specific case of an equilateral triangle formation. In this formation, each craft is assumed to have the same mass m and a common radial displacement r from the Hill-frame origin. The position of each spacecraft is specified by two values: a distance d_i in the $\hat{\boldsymbol{o}}_1$ direction, and a distance e_i in the $\hat{\boldsymbol{o}}_2$ direction. Because this formation must lie completely in one of the Hill-frame planes, the distance f_i in the $\hat{\boldsymbol{o}}_3$ direction is defined to be zero. Referring to Fig. 4, the positions of each spacecraft are prescribed as follows.

$$d_1 = r\cos(\theta) \qquad e_1 = r\sin(\theta) \qquad f_1 = 0 \tag{23a}$$

$$d_2 = r\cos(\theta + 2\pi/3) \qquad e_2 = r\sin(\theta + 2\pi/3) \qquad f_2 = 0 \tag{23b}$$

$$d_3 = r\cos(\theta + 4\pi/3) \qquad e_3 = r\sin(\theta + 4\pi/3) \qquad f_3 = 0 \tag{23c}$$

The center-of-mass condition is automatically satisfied by prescribing the positions of the equal-mass spacecraft to lie at the vertices of an equilateral triangle whose center coincides with the origin of the Hill frame. By evaluating the products of inertia as follows, the formation is shown to satisfy the principal axes condition.

$$I_{ef} = mr^2 \sum_{i=1}^{3} e_i f_i = 0 \tag{24}$$

$$I_{df} = mr^2 \sum_{i=1}^{3} d_i f_i = 0 \tag{25}$$

and

$$\begin{aligned} I_{de} &= mr^2 \sum_{i=1}^{3} d_i e_i = mr^2 \bigg[\cos\theta\sin\theta \\ &+ \cos\left(\theta + \frac{2\pi}{3}\right)\sin\left(\theta + \frac{2\pi}{3}\right) + \cos\left(\theta + \frac{4\pi}{3}\right)\sin\left(\theta + \frac{4\pi}{3}\right)\bigg] \\ &= mr^2\left[\cos^2\theta\left(-\frac{\sqrt{3}}{4} + \frac{\sqrt{3}}{4}\right) + \sin^2\theta\left(-\frac{\sqrt{3}}{4} + \frac{\sqrt{3}}{4}\right) \right. \\ &\left. + \cos\theta\sin\theta\left(1 + \frac{1}{4} - \frac{3}{4} + \frac{1}{4} - \frac{3}{4}\right)\right] = 0 \end{aligned} \tag{26}$$

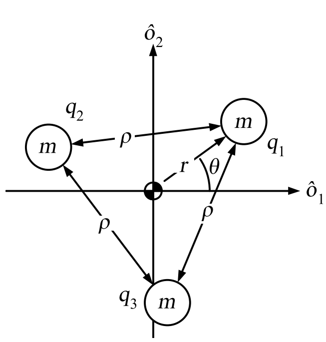

Fig. 4 Equilateral triangle spacecraft formation.

Just as in the case of an arbitrary three-spacecraft formation, there are six equations that must be satisfied to ensure that the spacecraft are stationary with respect to the Hill frame. These equations of motion are linear with respect to the charge products and can be represented in matrix form as

$$m\rho^3 \begin{bmatrix} a_d d_1 \\ a_d d_2 \\ a_d d_3 \\ a_e e_1 \\ a_e e_2 \\ a_e e_3 \end{bmatrix} = \begin{bmatrix} d_1 - d_2 & d_1 - d_3 & 0 \\ d_2 - d_1 & 0 & d_2 - d_3 \\ 0 & d_3 - d_1 & d_3 - d_2 \\ e_1 - e_2 & e_1 - e_3 & 0 \\ e_2 - e_1 & 0 & e_2 - e_3 \\ 0 & e_3 - e_1 & e_3 - e_2 \end{bmatrix} \begin{bmatrix} Q_{12} \\ Q_{13} \\ Q_{23} \end{bmatrix} \tag{27}$$

where ρ is the interspacecraft distance as seen in Fig. 4. Using simple trigonometry, the value of the triangle side length is found to be $\rho = 2r\cos(\pi/3) = r\sqrt{3}$.

To simplify the required open-loop charge analysis, all the positions d_i and e_i are written as the product of r and a trigonometric function of θ so that $d_i = r\tilde{d}_i(\theta)$ and $e_i = r\tilde{e}_i(\theta)$. The tilde functions are defined as

$$\tilde{d}_1(\theta) = \cos(\theta) \qquad \tilde{e}_1(\theta) = \sin(\theta) \tag{28a}$$

$$\tilde{d}_2(\theta) = \cos(\theta + 2\pi/3) \qquad \tilde{e}_2(\theta) = \sin(\theta + 2\pi/3) \tag{28b}$$

$$\tilde{d}_3(\theta) = \cos(\theta + 4\pi/3) \qquad \tilde{e}_3(\theta) = \sin(\theta + 4\pi/3) \tag{28c}$$

This definition is convenient because r can be factored out of the differences in position so that $d_i - d_j$ becomes $r(\tilde{d}_i - \tilde{d}_j)$. In this respect, the tilde functions define a nondimensional distance. The appropriate trigonometric identities are now employed to find the position differences between the spacecraft.

$$\tilde{d}_1 - \tilde{d}_2 = -\sqrt{3}\sin(\theta + 4\pi/3) \qquad \tilde{e}_1 - \tilde{e}_2 = \sqrt{3}\cos(\theta + 4\pi/3) \tag{29a}$$

$$\tilde{d}_1 - \tilde{d}_3 = \sqrt{3}\sin(\theta + 2\pi/3) \qquad \tilde{e}_1 - \tilde{e}_3 = -\sqrt{3}\cos(\theta + 2\pi/3) \tag{29b}$$

$$\tilde{d}_2 - \tilde{d}_3 = -\sqrt{3}\sin(\theta) \qquad \tilde{e}_2 - \tilde{e}_3 = \sqrt{3}\cos(\theta) \tag{29c}$$

Note the simple relationship that exists between the position differences and the positions themselves:

$$\tilde{d}_1 - \tilde{d}_2 = -\tilde{e}_3\sqrt{3} \qquad \tilde{e}_1 - \tilde{e}_2 = \tilde{d}_3\sqrt{3} \tag{30a}$$

$$\tilde{d}_1 - \tilde{d}_3 = \tilde{e}_2\sqrt{3} \qquad \tilde{e}_1 - \tilde{e}_3 = -\tilde{d}_2\sqrt{3} \tag{30b}$$

$$\tilde{d}_2 - \tilde{d}_3 = -\tilde{e}_1\sqrt{3} \qquad \tilde{e}_2 - \tilde{e}_3 = \tilde{d}_1\sqrt{3} \tag{30c}$$

Based upon these results, Eq. (27) can be rewritten in an elegantly simple form for the equilateral triangle special case:

$$m\rho^2 \begin{bmatrix} a_d\tilde{d}_1 \\ a_d\tilde{d}_2 \\ a_d\tilde{d}_3 \\ a_e\tilde{e}_1 \\ a_e\tilde{e}_2 \\ a_e\tilde{e}_3 \end{bmatrix} = \begin{bmatrix} -\tilde{e}_3 & \tilde{e}_2 & 0 \\ \tilde{e}_3 & 0 & -\tilde{e}_1 \\ 0 & -\tilde{e}_2 & \tilde{e}_1 \\ \tilde{d}_3 & -\tilde{d}_2 & 0 \\ -\tilde{d}_3 & 0 & \tilde{d}_1 \\ 0 & \tilde{d}_2 & -\tilde{d}_1 \end{bmatrix} \begin{bmatrix} Q_{12} \\ Q_{13} \\ Q_{23} \end{bmatrix} \tag{31}$$

As discussed in the analysis of the arbitrary triangular formation, the center-of-mass condition eliminates two equations, one for each direction, while the principal axes condition removes one more equation. To this end, the second, fourth, and sixth equations are removed. The remaining equations, as listed in Eq. (32), are used to solve for the charge products:

$$m\rho^2 \begin{bmatrix} a_d\tilde{d}_1 \\ -a_e\tilde{e}_2 \\ a_d\tilde{d}_3 \end{bmatrix} = \begin{bmatrix} -\tilde{e}_3 & \tilde{e}_2 & 0 \\ \tilde{d}_3 & 0 & -\tilde{d}_1 \\ 0 & -\tilde{e}_2 & \tilde{e}_1 \end{bmatrix} \begin{bmatrix} Q_{12} \\ Q_{13} \\ Q_{23} \end{bmatrix} \tag{32}$$

Solving for the required charge products yields

$$\begin{bmatrix} Q_{12} \\ Q_{13} \\ Q_{23} \end{bmatrix} = \frac{-m\rho^2}{\tilde{d}_1\tilde{e}_2\tilde{e}_3 - \tilde{e}_1\tilde{e}_2\tilde{d}_3} \begin{bmatrix} \tilde{d}_1\tilde{e}_2 & \tilde{e}_1\tilde{e}_2 & \tilde{d}_1\tilde{e}_2 \\ \tilde{e}_1\tilde{d}_3 & \tilde{e}_1\tilde{e}_3 & \tilde{d}_1\tilde{e}_3 \\ \tilde{e}_2\tilde{d}_3 & \tilde{e}_2\tilde{e}_3 & \tilde{e}_2\tilde{d}_3 \end{bmatrix} \begin{bmatrix} a_d\tilde{d}_1 \\ -a_e\tilde{e}_2 \\ a_d\tilde{d}_3 \end{bmatrix} \tag{33}$$

All that is left is to bring the solutions for the charge products to their simplest forms. For this task, the third equation is examined. After substituting Eqs. (28) into Eq. (33), multiplying, and using double and triple angle identities, the value of the charge product Q_{23} is represented in the surprisingly simple form of a sinusoidal function of 2θ with an amplitude and offset that are both functions of a_d and a_e:

$$Q_{23} = m\rho^2(a_e - a_d)\frac{\sqrt{3}}{3}\cos(2\theta) + m\rho^2(a_e + a_d)\frac{\sqrt{3}}{6} \tag{34}$$

A similar approach can be taken to find Q_{12} and Q_{13}, however, it is easier to recognize that each spacecraft is offset by 120 deg, and because the spacecraft are identical, the solutions for the charge products will only differ in phase angle as seen in the following equations.

$$Q_{12} = m\rho^2(a_e - a_d)\frac{\sqrt{3}}{3}\cos\left(2\theta + \frac{2\pi}{3}\right) + m\rho^2(a_e + a_d)\frac{\sqrt{3}}{6} \tag{35}$$

$$Q_{13} = m\rho^2(a_e - a_d)\frac{\sqrt{3}}{3}\cos\left(2\theta - \frac{2\pi}{3}\right) + m\rho^2(a_e + a_d)\frac{\sqrt{3}}{6} \tag{36}$$

These solutions are presented graphically in Fig. 5. Each subfigure shows the charge product solution for an equilateral triangle formation lying in one of the Hill-frame planes. Compared with the analytical equilateral triangle solutions in [7,12], these results are more general because they are valid for arbitrary formation orientation θ and alignment with any of the Hill-frame planes.

According to King et al. [7], sparse aperture interferometry requires that an array of sensors be distributed on the circumference of a planar circle. Although the static equilateral triangle formation is one of the simplest such formations, it may serve as a theoretical building block toward more complex formations. Such formations may include circular formations of large numbers of spacecraft or dynamic equilateral triangle formations that are capable of changing both size and orientation.

Again, although constant-charge products Q_{ij} can always be determined for the charged N-craft problem, it may be impossible to find constant individual spacecraft charges $\tilde{q}_i$ necessary to physically implement a formation. As an example, refer to Fig. 5. The subfigures display the charge products necessary to maintain a static equilateral triangle formation for any given orientation in the $\hat{\boldsymbol{o}}_r - \hat{\boldsymbol{o}}_\theta$, $\hat{\boldsymbol{o}}_r - \hat{\boldsymbol{o}}_h$, and $\hat{\boldsymbol{o}}_\theta - \hat{\boldsymbol{o}}_h$ planes. The gray areas in the subfigures indicate orientations that are physically unimplementable. From Fig. 5a, it can be seen that a static equilateral triangle formation can be implemented with any orientation in the $\hat{\boldsymbol{o}}_r - \hat{\boldsymbol{o}}_\theta$ orbit plane. Unfortunately, the $\hat{\boldsymbol{o}}_r - \hat{\boldsymbol{o}}_h$ plane and $\hat{\boldsymbol{o}}_\theta - \hat{\boldsymbol{o}}_h$ plane formations do not share this quality. In the $\hat{\boldsymbol{o}}_r - \hat{\boldsymbol{o}}_h$ orbit-normal plane, the equilateral triangle can only be implemented in certain ranges of θ. By a visual inspection of the charge products in Fig. 5b it can be seen that neither of the conditions outlined at the end of Sec. IV are met in the shaded areas; either one charge product is zero or one charge product is negative. By inserting the appropriate values for a_d and a_e

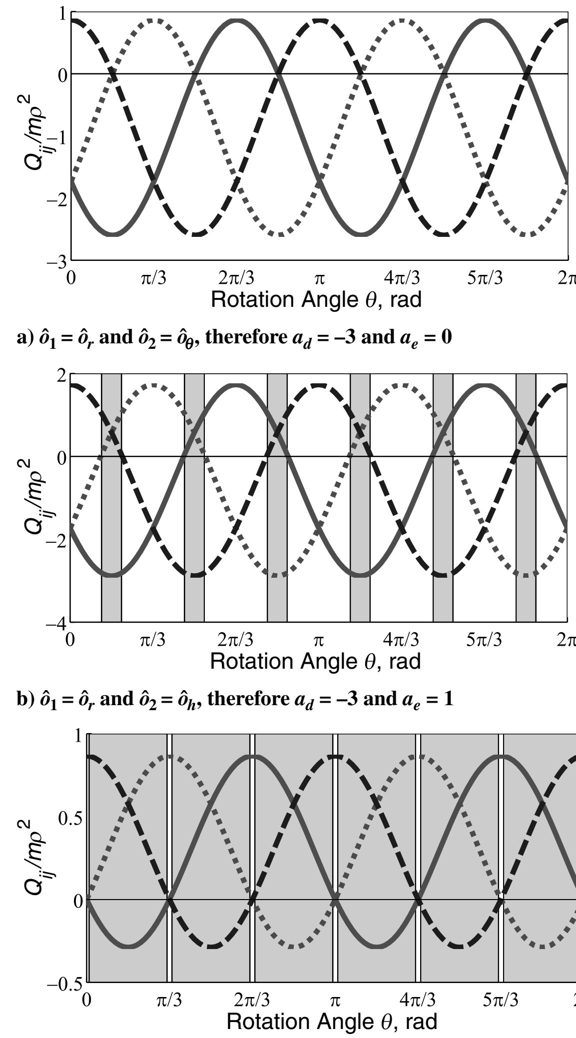

a) $\hat{o}_1 = \hat{o}_r$ and $\hat{o}_2 = \hat{o}_\theta$, therefore $a_d = -3$ and $a_e = 0$

b) $\hat{o}_1 = \hat{o}_r$ and $\hat{o}_2 = \hat{o}_h$, therefore $a_d = -3$ and $a_e = 1$

c) $\hat{o}_1 = \hat{o}_\theta$ and $\hat{o}_2 = \hat{o}_h$, therefore $a_d = 0$ and $a_e = 1$

Fig. 5 Q_{ij} for equilateral triangular formation aligned with different Hill-frame planes.

into the equations for the charge products and solving for the roots, the ranges in which a static formation is possible are found to be $-\phi + (m\pi/3) < \theta < \phi + (m\pi/3)$ where m is an integer and $\phi = \arctan[\sqrt{3}(-2 + \sqrt{5})]$. For the equilateral triangle formation in the $\hat{\boldsymbol{o}}_\theta - \hat{\boldsymbol{o}}_h$ local horizontal plane, static formations with constant charges are only possible at discrete values of θ where $\theta = m\pi/3$. This corresponds to equilateral triangle formations in which one of the spacecraft lie either on the $\hat{\boldsymbol{o}}_\theta$ axis or the $\hat{\boldsymbol{o}}_h$ axis.

VI. Arbitrary *N*-Craft Formations

A. Determination of Charge Products

The analysis that has been presented for constant-charge formations of two and three craft can be extended to the case of N-craft formations. Further, the charged plasma environment is taken into account by including the Debye length λ_d. In this environment, the Debye length once again becomes important and must therefore be reincorporated into the static equations as follows.

$$m_i\frac{\ddot{x}_i}{n^2} = 0 = 3x_i m_i + \sum_{j=1}^{N}\frac{x_i - x_j}{\rho_{ij}^3}\tilde{q}_i\tilde{q}_j e^{-\frac{\rho_{ij}}{\lambda_d}} \tag{37a}$$

$$m_i\frac{\ddot{y}_i}{n^2} = 0 = \sum_{j=1}^{N}\frac{y_i - y_j}{\rho_{ij}^3}\tilde{q}_i\tilde{q}_j e^{-\frac{\rho_{ij}}{\lambda_d}} \tag{37b}$$

$$m_i \frac{\ddot{z}_i}{n^2} = 0 = -z_i m_i + \sum_{j=1}^{N} \frac{z_i - z_j}{\rho_{ij}^3} \tilde{q}_i \tilde{q}_j e^{-\frac{\rho_{ij}}{\lambda_d}} \tag{37c}$$

If the notation presented in Sec. III.B is used, then Eqs. (37) can be represented compactly as

$$d_i = \frac{1}{m_i a_d} \sum_{j=1}^{N} \frac{d_i - d_j}{\rho_{ij}^3} \tilde{q}_i \tilde{q}_j e^{-\frac{\rho_{ij}}{\lambda_d}} \tag{38}$$

where d can be x, y, and z, $i = 1, \ldots, N$, and the summation does not include the case where $j = i$. Note that although the Debye exponential term is now included, the equations are still linear in the charge products, $Q_{ij} = \tilde{q}_i \tilde{q}_j$. For this reason, the equations that must be satisfied to ensure a static formation can be placed in matrix form as seen in the following equation.

$$\underbrace{\begin{bmatrix} d_1 \\ d_2 \\ d_3 \\ \vdots \\ d_N \\ e_1 \\ e_2 \\ e_3 \\ \vdots \\ e_N \\ f_1 \\ f_2 \\ f_3 \\ \vdots \\ f_N \end{bmatrix}}_{L} = \underbrace{\begin{bmatrix} D_{12} & D_{13} & D_{1,4,\ldots,N} & 0 & 0 & 0 & \cdots & 0 \\ -D_{12} & 0 & 0\cdots 0 & D_{23} & D_{24} & D_{2,5,\ldots,N} & \cdots & 0 \\ 0 & -D_{13} & 0\cdots 0 & -D_{23} & 0 & 0\cdots 0 & \cdots & 0 \\ \vdots & \vdots & \vdots & \vdots & \vdots & \vdots & \ddots & \vdots \\ 0 & 0 & 0\cdots 0 & 0 & 0 & 0\cdots 0 & \cdots & -D_{N-1,N} \\ E_{12} & E_{13} & E_{1,4,\ldots,N} & 0 & 0 & 0 & \cdots & 0 \\ -E_{12} & 0 & 0\cdots 0 & E_{23} & E_{24} & E_{2,5,\ldots,N} & \cdots & 0 \\ 0 & -E_{13} & 0\cdots 0 & -E_{23} & 0 & 0\cdots 0 & \cdots & 0 \\ \vdots & \vdots & \vdots & \vdots & \vdots & \vdots & \ddots & \vdots \\ 0 & 0 & 0\cdots 0 & 0 & 0 & 0\cdots 0 & \cdots & -E_{N-1,N} \\ F_{12} & F_{13} & F_{1,4,\ldots,N} & 0 & 0 & 0 & \cdots & 0 \\ -F_{12} & 0 & 0\cdots 0 & F_{23} & F_{24} & F_{2,5,\ldots,N} & \cdots & 0 \\ 0 & -F_{13} & 0\cdots 0 & -F_{23} & 0 & 0\cdots 0 & \cdots & 0 \\ \vdots & \vdots & \vdots & \vdots & \vdots & \vdots & \ddots & \vdots \\ 0 & 0 & 0\cdots 0 & 0 & 0 & 0\cdots 0 & \cdots & -F_{N-1,N} \end{bmatrix}}_{M} \underbrace{\begin{bmatrix} Q_{12} \\ Q_{13} \\ Q_{1,4,\ldots,N} \\ Q_{23} \\ Q_{24} \\ Q_{2,5,\ldots,N} \\ \vdots \\ Q_{N-1,N} \end{bmatrix}}_{Q} \tag{39}$$

where

$$D_{ij} = \frac{1}{m_i a_d} \frac{d_i - d_j}{\rho_{ji}^3} e^{-\frac{\rho_{ij}}{\lambda_d}} \tag{40a}$$

$$E_{ij} = \frac{1}{m_i a_e} \frac{e_i - e_j}{\rho_{ji}^3} e^{-\frac{\rho_{ij}}{\lambda_d}} \tag{40b}$$

$$F_{ij} = \frac{1}{m_i a_f} \frac{f_i - f_j}{\rho_{ji}^3} e^{-\frac{\rho_{ij}}{\lambda_d}} \tag{40c}$$

The values of $\boldsymbol{L}$ and $\boldsymbol{M}$ are known. Using the pseudoinverse for $\boldsymbol{M}$, a solution is found for $\boldsymbol{Q}$ which satisfies Eq. (39). The minimum norm solution for $\boldsymbol{Q}$ is of the form

$$\boldsymbol{Q}^* = \boldsymbol{M}^T (\boldsymbol{M}\boldsymbol{M}^T)^{-1} \boldsymbol{L} \tag{41}$$

and any arbitrary solution for the charge product vector $\boldsymbol{Q}$ can then be written as

$$\boldsymbol{Q} = \boldsymbol{Q}^* + \mathrm{Null}(\boldsymbol{M})\boldsymbol{t} \tag{42}$$

where $\boldsymbol{t}$ represents a parameter vector with as many elements as there are basis vectors in the null space of $\boldsymbol{M}$.

In Sec. III.A, it is shown that due to the center-of-mass and principal axes conditions, six of the equations displayed Eq. (39) are redundant. The issue of equation redundancy is now discussed for the specific cases of one-, two-, and three-dimensional formations.

For one-dimensional, axially aligned formations, all of the distances e_i and f_i will be zero. Therefore, from Eq. (39), all the rows of $\boldsymbol{M}$ with elements E_{ij} and F_{ij} will be populated by only zeros. These rows add no new information and can be removed. The center-of-mass condition applies one more constraint that insures the formation center of mass is located at the origin. Because the formation spacecraft positions have already been chosen to satisfy this condition, one more equation is redundant and one more row may be removed from $\boldsymbol{M}$.

For two-dimensional, planar formations aligned with the Hill frame, the distances f_i will be zero so that all corresponding rows of $\boldsymbol{M}$ can be removed. The center-of-mass condition can be used to remove two more equations, whereas the principal axes condition can be used to remove one more. The choice of which equations to remove is somewhat arbitrary so long as rank is preserved while removing the rows of $\boldsymbol{M}$. For instance, removing three rows corresponding to d_1, d_2, and d_3 would decrease the rank of $\boldsymbol{M}$ by one, however, the rows corresponding to d_1, d_2, and e_1 could be removed with no decrease in rank.

Finally, the center-of-mass condition is used to eliminate three equations, whereas the principal axes conditions are used to eliminate three additional equations. However, again, care must be taken so that the rank of $\boldsymbol{M}$ is preserved as the rows are removed. Although the choice is still somewhat arbitrary, it is recommended the rows corresponding with d_N, e_{N-1}, e_N, f_{N-2}, f_{N-1}, and f_N be removed from $\boldsymbol{M}$. This will always ensure that the rank of $\boldsymbol{M}$ is maintained.

B. Relationship Between Charge Products and Charges

Because constant-charge static Coulomb formations will ultimately be implemented with the charges q_i rather than the charge products Q_{ij}, it is important to completely understand the relationship that exists between the charges and charge products. For the simple case of two spacecraft, there is one charge product and two charges. There can therefore be infinite charge solutions of the form $\tilde{q}_1 = Q_{12}/\tilde{q}_2$ in which $\tilde{q}_2$ can be arbitrarily chosen. For the case of a three-spacecraft triangular formation, there are three charge products

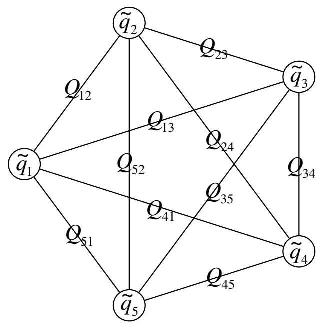

Fig. 6 Graphical representation of the relationship between charges and charge products.

and three charges. A solution can always be found for these charges from the charge products, however, these charges may be imaginary and therefore unimplementable. For more than three spacecraft, the number of charge products is always larger than the number of craft charges. Generally speaking, for N spacecraft there will be $N(N-1)/2$ charge products Q_{ij} and only N charges q_i. Because of this, for more than three craft, it is difficult to determine implementable charging solutions from the charge products. However, this *does not* indicate that constant-charge formations of more than three craft cannot exist. Earlier analytical and numerical works have shown that these formations in fact *do* exist [6,7,12,16], however, these formations exist in a small subset of all possible spacecraft position and mass configurations.

Figure 6 is a graphical representation of the relationship between spacecraft charges and charge products in a formation. To begin to understand this relation, recall that $Q_{ij} = \tilde{q}_i\tilde{q}_j$, therefore $\tilde{q}_1 = Q_{12}/\tilde{q}_2$. From Fig. 6, the latter equation corresponds to moving from $\tilde{q}_1$ through Q_{12} to $\tilde{q}_2$. Similarly, starting at $\tilde{q}_2$ and moving to $\tilde{q}_3$ yields $\tilde{q}_2 = Q_{23}/\tilde{q}_3$, and starting at $\tilde{q}_3$ and moving to $\tilde{q}_1$ yields $\tilde{q}_3 = Q_{31}/\tilde{q}_1$. Combining these three equations yields

$$\tilde{q}_1^{\,2} = \frac{Q_{12}Q_{31}}{Q_{23}} \tag{43}$$

This equation corresponds to a path that starts at $\tilde{q}_1$ and moves through $\tilde{q}_2$ and $\tilde{q}_3$ and then stops at $\tilde{q}_1$. Notice that the Q_{ij} crossed during the odd steps (e.g., Q_{12} and Q_{31}) are in the numerator, whereas the Q_{ij} crossed during the even steps (e.g., Q_{23}) are in the denominator. In this manner, an equation can be formed for any path through the graph. Equation (43) represents one condition that q_1 must satisfy. By taking alternate paths through the graph, more conditions can be found as enumerated in Table 1.

At this point, one might conclude that besides the triangular loops listed in Table 1, one might find many other loops leading to more and more equations that q_1 must satisfy. Fortunately, this is not the case. For instance, the path around the outside of the pentagon,

Table 1 Enumeration of loop equations for $\tilde{q}_1$

Eq. no.	Path	Loop equation
1	$\tilde{q}_1 - \tilde{q}_2 - \tilde{q}_3 - \tilde{q}_1$	$\tilde{q}_1^{\,2} = \frac{Q_{12}Q_{31}}{Q_{23}}$
2	$\tilde{q}_1 - \tilde{q}_2 - \tilde{q}_4 - \tilde{q}_1$	$\tilde{q}_1^{\,2} = \frac{Q_{12}Q_{41}}{Q_{24}}$
3	$\tilde{q}_1 - \tilde{q}_2 - \tilde{q}_5 - \tilde{q}_1$	$\tilde{q}_1^{\,2} = \frac{Q_{12}Q_{51}}{Q_{25}}$
4	$\tilde{q}_1 - \tilde{q}_3 - \tilde{q}_4 - \tilde{q}_1$	$\tilde{q}_1^{\,2} = \frac{Q_{13}Q_{41}}{Q_{34}}$
5	$\tilde{q}_1 - \tilde{q}_3 - \tilde{q}_5 - \tilde{q}_1$	$\tilde{q}_1^{\,2} = \frac{Q_{13}Q_{51}}{Q_{35}}$
6	$\tilde{q}_1 - \tilde{q}_4 - \tilde{q}_5 - \tilde{q}_1$	$\tilde{q}_1^{\,2} = \frac{Q_{14}Q_{51}}{Q_{45}}$

starting from $\tilde{q}_1$, moving through $\tilde{q}_2$, $\tilde{q}_3$, $\tilde{q}_4$, and $\tilde{q}_5$, and then stopping again at $\tilde{q}_1$, would produce the equation $\tilde{q}_1^2 = (Q_{12}Q_{34}Q_{51})/(Q_{23}Q_{45})$. This equation is automatically satisfied by multiplying the first and sixth equations from Table 1 and then dividing by the fourth equation. In a similar manner, any loop that traverses more than three edges can be represented by a combination of loops that only cross three edges. For this reason, the number of equations that a charge must satisfy is equal to the number of unique triangular loops that pass through the charge's node. From Fig. 6, it is apparent that the number of equations $\tilde{q}_1$ must satisfy is equal to $(N-1)(N-2)/2$. Therefore, to have an implementable formation, the charge of each spacecraft q_i must satisfy $(N-1)(N-2)/2$ equations. If these equations are contradictory to one another, as will often be the case, then there is no way to physically implement the formation with constant charges. In the event that the equations are *not* self-contradictory, they still must satisfy the criteria outlined at the end of Sec. IV to ensure that the charges are finite and real valued. Although the geometry and mass distribution necessary for a formation to be implementable are not obvious as of yet, further analysis may give insight into analytically determining families of geometries and mass distributions that lead to formations implementable by constant charge.

C. Pulse-Width Modulation

Formations need not be implemented only with constant charges. Pulse-width modulation is a promising prospective method for controlling Coulomb formations and for overcoming the issues inherent with constant-charge implementations. Roughly, pulse-width modulation is a method by which the charges of individual spacecraft are rapidly modulated between charged and not-charged states, or pulsed, such that the net effective charge product over a duty cycle between any two spacecraft is equivalent to the charge product necessary to maintain a stationary formation in the Hill frame. The charge product solutions developed in earlier sections provide the required net charges that must be applied to a pulse-width modulated implementation. However, rapidly changing the electrostatic potentials of the spacecraft raises technical challenges in implementing Coulomb propulsion which must be addressed. For example, the rapid charge transfer across the vehicle necessary to implement pulse-width modulation control will greatly increase the associated electrical power and dispelled charge mass consumption (for the positive ion discharge case). Constant-charge solutions are simpler to implement, and more powerful and fuel efficient, but the associated formation geometries are more restricted.

VII. Conclusions

To implement a constant-charge Coulomb formation, it is important to first determine the nominal charge values necessary to sustain the formation. Once determined, these values can be used as open-loop, feed-forward charges in stabilizing feedback control laws. The results of this paper bring the state of the art one step closer to determining necessary charge solutions for any feasible two- and three-craft formations. Specifically, a method is outlined by which a charge product solution can be determined for any formation that fulfills the center-of-mass and principal axes conditions. The charge products are then related to the constant spacecraft charges necessary to maintain a static Coulomb formation. However, for a general N-craft formation, it is not always possible to find real-valued, finite valued, or single-valued charges. Criteria are developed in this paper that will indicate whether or not a formation will have real, finite charges.

Although in its infancy, the study of Coulomb formation control is proving to be a rich field of research. Coulomb formations may hold answers to many of the logistical concerns that plague close-proximity flying today [7]. However, with each question that is answered, several more interesting questions arise. Future research will therefore be directed toward many different areas. Among the areas of future interest are stability and controllability of various Coulomb formations, control via pulse-width modulation, considerations of finite-sized craft (currently, models considered are point charges and point masses), and finally, dynamic, periodic formations.

Acknowledgment

The authors would like to acknowledge fruitful discussions with Mark L. Psiaki on using pulse-width modulation to control static Coulomb formations.

References

[1] Mullen, E. G., Gussenhoven, M. S., and Hardy, D. A., "SCATHA Survey of High-Voltage Spacecraft Charging in Sunlight," *Journal of the Geophysical Sciences*, Vol. 91, No. A2, 1986, pp. 1474–1490.

[2] Whipple, E. C., and Olsen, R. C., "Importance of Differential Charging for Controlling Both Natural and Induced Vehicle Potentials on ATS-5 and ATS-6," *Proceedings of the 3rd Spacecraft Charging Technology Conference*, NASA CP 2182, 1980, p. 887.

[3] Torkar, K., Riedler, W. , Fehringer, M., Rüdenauer, F., Escoubet, C. P., Arends, H., Narheim, B. T., Svenes, K., McCarthy, M. P., Parks, G. K., Lin, R. P., and Rème, H., "Spacecraft Potential Control Aboard Equator-S as a Test for Cluster-II," *Annales Geophysicae*, Vol. 17, No. 12, 1999, pp. 1582–1591.

[4] Schmidt, R, Arends, H., Pedersen, A., Rüdenauer, F., Fehringer, M., Narheim, B. T., Svenes, R., Kvernsveen, K., Tsuruda, K., Mukai, T., Hayakawa, H., and Nakamura, M., "Results from Active Spacecraft Potential Control on the Geotail Spacecraft," *Journal of Geophysical Research*, Vol. 100, No. A9, 1995, pp. 253–259.

[5] Torkar, K., Riedler, W., Escoubet, C. P., Fehringer, M., Schmidt, R., Grard, R. J. L., Arends, H., Rüdenauer, F., Steiger, W., Narheim, B. T., Svenes, K., Torbert, R., André, M., Fazakerley, A., Goldstein, R., Olsen, R. C., Pedersen, A., Whipple, E., and Zhao, H., "Active Spacecraft Potential Control for Cluster-Implementation and First Results," *Annales Geophysicae*, Vol. 19, Nos. 10–12, 2001, pp. 1289–1302.

[6] King, L. B., Parker, G. G., Deshmukh, S., and Chong, J.-H., "Study of Interspacecraft Coulomb Forces and Implications for Formation Flying," *Journal of Propulsion and Power*, Vol. 19, No. 3, May–June 2003, pp. 497–505.

[7] King, L. B., Parker, G. G., Deshmukh, S., and Chong, J.-H., "Spacecraft Formation-Flying Using Inter-Vehicle Coulomb Forces," NASA/NASA Inst. for Advanced Concepts Tech. Rept., http://www.niac.usra.edu, 2002.

[8] Natarajan, A., and Schaub, H., "Linear Dynamics and Stability Analysis of a Coulomb Tether Formation," *AAS Space Flight Mechanics Meeting*, American Astronautical Society Paper 05-204, 2005.

[9] Gombosi, T. I., *Physics of the Space Environment*, Cambridge Univ. Press, Cambridge, England, U.K., 1998.

[10] Schaub, H., and Parker, G. G., "Constraints of Coulomb Satellite Formation Dynamics, Part 1: Cartesian Coordinates," *Journal of Celestial Mechanics and Dynamical Astronomy* (submitted for publication), 2004.

[11] Schaub, H., and Kim, M., "Orbit Element Difference Constraints for Coulomb Satellite Formations," *AIAA/AAS Astrodynamics Specialist Conference*, AIAA Paper 04-5213, 2004.

[12] Schaub, H., Parker, G. G., and King, L. B., "Challenges and Prospect of Coulomb Formations," *AAS John L. Junkins Astrodynamics Symposium*, American Astronautical Society Paper 03-278, 2003.

[13] Schaub, H., Hall, C., and Berryman, J., "Necessary Conditions for Circularly-Restricted Static Coulomb Formations," *AAS Malcolm D. Shuster Astronautics Symposium*, American Astronautical Society Paper 05-472, 2005.

[14] Schaub, H., "Stabilization of Satellite Motion Relative to a Coulomb Spacecraft Formation," *Journal of Guidance, Control, and Dynamics*, Vol. 28, No. 6, Nov.–Dec. 2005, pp. 1231–1239.

[15] Parker, G. G., Passerello, C. E., and Schaub, H., "Static Formation Control Using Interspacecraft Coulomb Forces," Paper 20060048514.

[16] Berryman, J., and Schaub, H., "Static Equilibrium Configurations in GEO Coulomb Spacecraft Formations," *AAS Spaceflight Mechanics Meeting*, American Astronautical Society Paper 05-104, 2005.

[17] Hill, G. W., "Researches in the Lunar Theory," *American Journal of Mathematics*, Vol. 1, No. 1, 1878, pp. 5–26.

[18] Clohessy, W. H., and Wiltshire, R. S., "Terminal Guidance System for Satellite Rendezvous," *Journal of the Aerospace Sciences*, Vol. 27, No. 9, Sept. 1960, pp. 653–658.

[19] Schaub, H., and Junkins, J. L., *Analytical Mechanics of Space Systems*, AIAA Education Series, AIAA, Reston, VA, October 2003.

[20] Natarajan, A., and Schaub, H., "Linear Dynamics and Stability Analysis of a Coulomb Tether Formation," *Journal of Guidance, Control, and Dynamics*, Vol. 29, No. 4, 2006, pp. 831–839.